Supporting Information for "Halogen activation and radical cycling initiated by imidazole-2-carboxaldehyde photochemistry"

Pablo Corral Arroyo[1,2], Raffael Aellig[3], Peter A. Alpert[1], Rainer Volkamer[4, 5], Markus Ammann[1]*

[1] Paul Scherrer Institute, Laboratory of Environmental Chemistry, 5232 Villigen PSI, Switzerland.

[2] Department of Chemistry and Biochemistry, University of Bern, 2012 Bern, Switzerland.

[3] ETH Swiss Federal Institute of Technology Zürich, Institute for Atmospheric and Climate Science, 8006, Zurich, Switzerland.

[4] Department of Chemistry and Biochemistry, 215 UCB, University of Colorado, Boulder, CO 80309, USA

[5] Cooperative Institute for Research in Environmental Sciences (CIRES), 216 UCB, University of Colorado, Boulder, CO 80309, USA

***markus.ammann@psi.ch** Ph: +41 56 310 4049, Paul Scherrer Institute

In total 10 pages, 4 figures and 1 tables.

1. Spectra

The absorption spectra for imidazole-2-carboxaldehyde (IC) (Corral-Arroyo et al., 2018) and citric acid (CA) are shown together with the irradiance of the lamps used and the solar irradiance for the surface of the Earth at 48° zenith angle (Figure S1). The irradiance spectra of the lamps overlaps with the absorption spectra of IC but not with the absorption spectra of CA. Therefore, IC is the primary chromophore in the system.

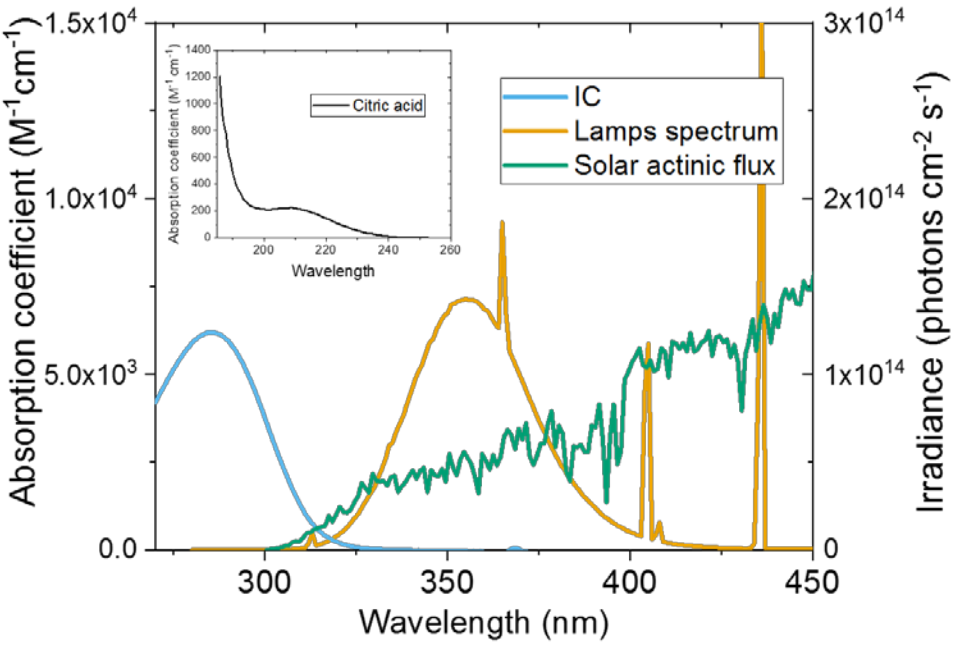

Figure S1. Absorption spectra of IC (100 mM) and CA (from NIST Chemistry WebBook), the irradiance spectrum of the UV lamps used and the solar irradiance spectra at 48° zenith angle.

2. NO loss and conversion to HO_2 production

NO was added to the gas flow in sufficient excess so that it acts as the scavenger for HO_2. A clear NO loss is detected upon switching on UV lights (Fig. S2) due to the release of HO_2 radicals into the gas phase and reaction of NO with HO_2 to form NO_2 and OH radical. OH is scavenged by NO to produce HONO. The chemiluminescence detector was preceded by a HONO trap with an optional bypass, and a molybdenum converter kept at 360°C, also with an optional bypass, to convert HONO and NO_2 into NO. This configuration allowed determining NO, NO_2 and HONO independently by differential measurements (Fig. S2 and S3). As in previous experiments (González Palacios et al., 2016), the ratio NO_2/HONO was about 1.4. The presence of HONO confirms that HO_2 was indeed the oxidant of NO, rather than another RO_2 species. The fact that the ratio to NO_2 is less than one indicates that some of the OH radicals may be lost at the surface in spite of the large NO concentration or that some HONO may decompose heterogeneously over the film or along tubing downstream of the CWFT. NO was added with a third flow of 5-10 ml/min of 100ppm NO in N_2. The NO concentration during CWFT experiments was always in excess of 10^{13} molecule cm^{-3} to efficiently scavenge 99% of HO_2 produced by the films within at most 50 ms (k_1 =8.0·10^{-12} cm^3 $molecule^{-1}$ s^{-1} at 298 K (Atkinson et al., 2004); $t_{99\%} = \frac{-\ln(0.01)}{k_1[NO]}$).

$$NO + HO_2 \rightarrow NO_2 + OH \quad (1)$$

The reaction between OH and iodine (k = 2.1 × 10^{-10} cm^3 $molecule^{-1}$ s^{-1}) can interfere with the reaction between OH and NO just at high concentrations of iodide (>0.001 M) when the iodine concentration may reach levels of 10^{11} - 5 × 10^{12} molecules cm^{-3}.

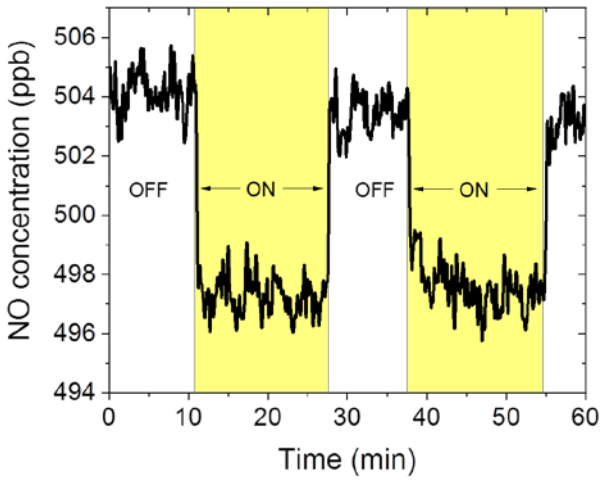

Figure S2. NO concentration raw data from films with lamps on (marked with yellow shading) and off at 35% RH and containing 4 mg of IC and 76.8 mg of CA with an iodide concentration of 1.3×10^{-5} M.

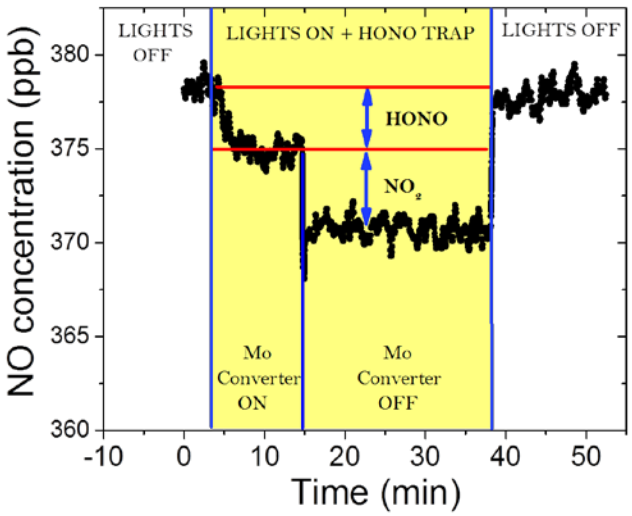

Figure S3. NO concentration raw data to show NO loss with lights on and HONO trap in line, and w/o the molybdenum converter, to allow differentiating between the NO loss resulting from the reaction with HO2 and the secondary loss from the reaction with OH. The film used contained 4 mg of IC and 76.8 mg of CA equilibrated to 40% RH, as in Corral-Arroyo et al. (2018).

3. I_2O_5 particle measurements

The measurement of the mass of I_2O_5 was performed by using a Scanning Mobility Particle Syzer (SMPS) consisting of a custom-built Differential Mobility Analyzer (DMA) and a Condensation Particle Counter (CPC, Model 3775). The mass size distribution is shown in Fig. S4 for different times. Particles below 20 nm in diameter could not be reliably measured.

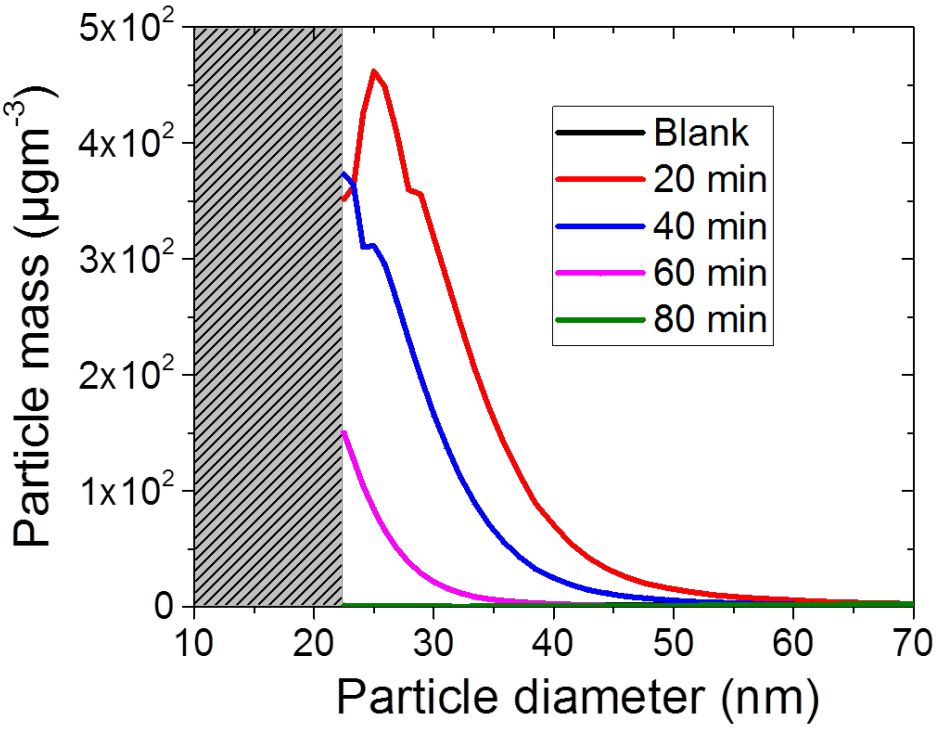

Figure S4. Mass size distribution of I_2O_5 particles produced from the oxidation of I_2 released at different times. The shady zone corresponds to the zone of the distribution we could not measure due to the limitations of the SMPS system.

4. Modelling

All reactions considered in the model and the corresponding rate coefficients are listed in Table S1. The excitation rate (R1) was obtained by integration of the product of the spectrum of the UV lamps with the absorption spectrum of IC (Figure S1). We used an intersystem crossing efficiency equal to 1.0 for IC, which had been previously observed in triplet forming chromophores (Lamola and Hammond, 1965). The rate coefficient of the quenching of the triplet (R2) by O_2 was approximated from Canonica et al. (Canonica, 2000). Values of rate coefficients for R3 and R4 are explained in detail in our previous work (Corral-Arroyo et al., 2018), and we note that they were optimized to agree with the measurements in the humidity range of 35±2 % RH, overlapping with the RH range of the present study. The rate coefficients of the reaction between the triplet of IC and iodide and bromide (R5) were taken from Tinel et al. (Tinel et al., 2014). Maillard et al. (Maillard et al., 1983) determined the rate coefficients of reactions between organic radicals and oxygen to be within (1-5) × 10^9 M^{-1} s^{-1}, justifying our estimate for the rate coefficient for the reaction between the ketyl radical and O_2 (R6) to be 10^9 M^{-1} s^{-1}. The rate coefficient of the reaction of HO_2 with itself (R7) was taken from Bielski et al. (Bielski et al., 1985). We used fixed rate coefficients for reactions R8-R11 (Bianchini and Chiappe, 1992; Ishigure et al., 1988; Morrison et al., 1971; Nagarajan and Fessenden, 1985). The reactions R12-R16 between HO_2 and halides species ($X^{\bullet}$, X_2^-, X_2) from previous literature (Bielski et al., 1985; Ishigure et al., 1988; Schwarz and Bielski, 1986; Wagner and Strehlow, 1987) were adjusted to obtain a better fit with our experimental data. This tuning is reasonable since protic solvents increase the rate coefficients of reaction involving radicals or excited states, whereas organic solvents do not affect those reactions. There is evidence that hydrogen bonded transition states are involved in electron transfer (IvkovicJensen and Kostic, 1997), proton coupled electron transfer, hydrogen abstraction reactions

(Mitroka et al., 2010) and quenching reactions between triplets and salts (Kunze et al., 1997). We assumed that the rate coefficient of the reaction between HO_2 and $I^{\bullet}$ and the reaction between HO_2 and I_2^- to give O_2 and iodide are equal to the one of the reaction between HO_2 and I_2^- to give HO_2^-. We considered the rate coefficient of the reaction between $Br_2^{\bullet-}$ and $Br^{\bullet}$ equals the one of the self-reaction of $Br^{\bullet}$. We assumed that X_3^- has the same reactivity as X_2. The photolysis rate of iodine was calculated by integrating the irradiance spectrum (Fig. S1) and the iodine photolysis spectrum (Choi et al., 2012) resulting in a rate of 0.01 s^{-1} (R17).

D_{HO2} was set to 3.5×10^{-12} cm^2 s^{-1}, estimated using data of HO_2 production in absence of halides as a function of film thickness (Corral-Arroyo et al., 2018). This value is about two orders of magnitude higher than that based on D_{H2O} data of Lienhard et al. (Lienhard et al., 2014). Assuming that D is inversely proportional to the radius of the diffusing molecule (Stokes-Einstein, eq. 1), we made a prediction of D_{Br2} and D_{I2} , leading to $D_{Br2} = 3 \times 10^{-12}$ cm^2 s^{-1} and $D_{I2} = 2 \times 10^{-12}$ cm^2 s^{-1} following the equation

$$D = \frac{k_B T}{6\pi\eta r}. \quad \text{(Eq. 1)}$$

Equation 1 shows the Stokes-Einstein relation, where k_B is the Boltzmann constant, T is temperature, η is viscosity and r is the apparent radius of the molecule that diffuses. Following our previous work (Corral-Arroyo et al., 2018), we represented the release due to diffusion by a simple first order loss rate coefficient (k_{diff}) as:

$$k_{diff} = \frac{D}{Film\ thickness}$$

Table S1. Chemical reactions and the corresponding rate coefficients used for the model in comparison to the literature values.

Reaction number	Rate coefficient	Reaction	Rate coefficient ($M^{-1}s^{-1}$) (Br/I) - Model	Rate coefficient ($M^{-1}s^{-1}$) (Br/I) - Reference	Reference
R1	k_{IC}	$IC \xrightarrow{h\nu} IC^{3*}$	$1 \cdot 10^{-3}$	$1 \cdot 10^{-3}$	Corral-Arroyo
R2	k_{scav-t}	$IC^{3*} + O_2 \rightarrow IC + {}^1O_2$	$3 \cdot 10^{9}$	$2.6 \cdot 10^{9}$	Canonica
R3	k_{decay}	$IC^{3*} \rightarrow IC$	$6.5 \cdot 10^{5}$	$6.5 \cdot 10^{5}$	Corral-Arroyo
R4	k_{CA}	$IC^{3*} + CA \rightarrow ICH + CA^{\bullet}$	90	90	Corral-Arroyo
R5	k_{hal}	$IC^{3*} + X^{-} \rightarrow ICH + X^{\bullet}$	$6.27 \cdot 10^{6}/5.33 \cdot 10^{9}$	$6.27 \cdot 10^{6}/5.33 \cdot 10^{9}$	Tinel
R6	k_{ICH}	$ICH + O_2 \rightarrow IC + HO_2$	$1 \cdot 10^{9}$	$1\text{-}5 \cdot 10^{9}$	Maillard
R7	k_{HO2}	$HO_2 + HO_2 \rightarrow H_2O_2 + O_2$	$8 \cdot 10^{5}$	$8.3 \cdot 10^{5}$	Bielski
R8	k_{x1}	$X^{\bullet} + X^{-} \rightarrow X_2^{-\bullet}$	$9 \cdot 10^{9}/1.1 \cdot 10^{10}$	$9 \cdot 10^{9}/1.1 \cdot 10^{10}$	Nagarajan/Ishigure
R9	k_{x2}	$X_2^{-\bullet} + X^{\bullet} \rightarrow X_3^{-}/X_2$	$8.4 \cdot 10^{9}/8.4 \cdot 10^{9}$	$-/8.4 \cdot 10^{9}$	Ishigure
R10	k_{x3}	$X^{\bullet} + X^{\bullet} \rightarrow X_2$	$3 \cdot 10^{9}/1.9 \cdot 10^{10}$	$-/1.9 \cdot 10^{10}$	Ishigure
R11	K_{eq}	$X_2 + X^{-} \leftrightarrow X_3^{-}$	$2.7 \cdot 10^{4\,E}/768^{E}$	$2.7 \cdot 10^{4\,E}/768^{E}$	Bianchini/Morrison
R12	k_{scav1}	$HO_2 + X^{\bullet} \rightarrow O_2 + HX$	$6 \cdot 10^{3}/5 \cdot 10^{6}$	$1.6 \cdot 10^{8}/-$	Wagner
R13	k_{scav2}	$HO_2 + X_2^{-\bullet} \rightarrow O_2 + 2\,X^{-} + H^{+}$	$6 \cdot 10^{3}/5 \cdot 10^{6}$	$1 \cdot 10^{8}/-$	Wagner
R14	k_{scav3}	$HO_2 + X_2^{-\bullet} \rightarrow HO_2^{-} + X_2$	$6 \cdot 10^{3}/5 \cdot 10^{6}$	$9.1 \cdot 10^{7}/4 \cdot 10^{9}$	Wagner/Ishigure
R15	k_{scav4}	$HO_2 + X_2 \rightarrow O_2 + X_2^{-\bullet} + H^{+}$	$6 \cdot 10^{3}/1 \cdot 10^{5}$	$1.5 \cdot 10^{8}/1.8 \cdot 10^{7}$	Bielski/Schwarz
R16	k_{scav4}	$HO_2 + X_3^{-} \rightarrow O_2 + X_2^{-\bullet} + H^{+} + X^{-}$	$6 \cdot 10^{3}/1 \cdot 10^{5}$	-/-	
R17	k_{scav5}	$X_2 \xrightarrow{h\nu} 2\,X^{\bullet}$	-/0.01	-/0.01	Calculated/Choi

Source of rate coefficients: (Bianchini and Chiappe, 1992; Bielski et al., 1985; Canonica, 2000; Choi et al., 2012; Corral-Arroyo et al., 2018; Ishigure et al., 1988; Maillard et al., 1983; Morrison et al., 1971; Nagarajan and Fessenden, 1985; Schwarz and Bielski, 1986; Tinel et al., 2014; Wagner and Strehlow, 1987) *First order rate coefficient. ^{E}Equilibrium constant

The differential equations shown below were used to model the concentration of the different chemical species and the production and release of HO_2 for several conditions assuming steady state.

$$\left(\frac{\mathbf{d[IC^{3*}]}}{\mathbf{dt}}\right) = \mathbf{k_{IC}[IC] - k_{decay}[IC^{3*}] - k_{scav-t}[O_2][IC^{3*}] - k_{CA}[CA][IC^{3*}] - k_{hal}[X^-][IC^{3*}]} = \mathbf{0}$$

$$\left(\frac{\boldsymbol{d[ICH]}}{\boldsymbol{dt}}\right) = \boldsymbol{k_{CA}[CA][IC^{3*}] + k_{hal}[X^-][IC^{3*}] - k_{1ICH}[O_2][ICH] - k_{scav1}[X^-][ICH] = 0}$$

$$\boldsymbol{[IC^{3*}] = \frac{k_{IC}[IC]}{k_{decay} + k_{scav-t}[O_2] + k_{CA}[CA] + k_X[X^-]}}$$

$$\boldsymbol{[ICH] = \frac{k_{CA}[CA][IC^{3*}] + k_{syr}[X^-][IC^{3*}]}{k_1[O_2]}}$$

$$\left(\frac{\boldsymbol{d[HO_2]}}{\boldsymbol{dt}}\right) = \boldsymbol{k_{ICH}[O_2][ICH] - k_{scav1}[X^\bullet][HO_2] - k_{scav2}[X^-][HO_2] - k_{scav3}[X_2^-][HO_2] - k_{scav4}[X_2^-][HO_2] - 2k_{HO2}[HO_2]^2 - k_{diff}[HO_2] = 0}$$

$$\left(\frac{\mathbf{d[X^\bullet]}}{\boldsymbol{dt}}\right) = \mathbf{k_X[X^-][IC^{3*}]} - \boldsymbol{k_{x1}[X^\bullet][X^-] - k_{x2}[X_2^-][X^\bullet] - k_{x3}[X^\bullet]^2 - k_{scav1}[X^\bullet][HO_2] = 0}$$

$$\left(\frac{\boldsymbol{d[X_2^-]}}{\boldsymbol{dt}}\right) = \boldsymbol{k_{x1}[X^\bullet][X^-] - k_{x2}[X_2^-][X^\bullet] - k_{scav2}[X_2^-][HO_2] - k_{scav3}[X_2^-][HO_2] + k_{scav4}[X_2][HO_2] = 0}$$

$$\left(\frac{\boldsymbol{d[X_2]}}{\boldsymbol{dt}}\right) = \boldsymbol{k_{x3}[X^\bullet]^2 + k_{x2}[X_2^-][X^\bullet] + k_{scav2}[X_2^-][HO_2] + k_{scav4}[X_2][HO_2] - k_{diff2}[X_2] - k_{scav5}[X_2] = 0}$$

References

Atkinson, R., Baulch, D. L., Cox, R. A., Crowley, J. N., Hampson, R. F., Hynes, R. G., Jenkin, M. E., Rossi, M. J., and Troe, J.: Evaluated kinetic and photochemical data for atmospheric chemistry: Volume I - gas phase reactions of O_x, HO_x, NO_x and SO_x species, Atmos. Chem. Phys., 4, 1461-1738, 2004.

Bianchini, R. and Chiappe, C.: Stereoselectivity and reversibility of electrophylic bromine addition to stilbenes in chloroform - Influence of bromide tribromide pentabromide equilibrium in the counteranion of the ionic intermediates, J. Org. Chem., 57, 6474-6478, 1992.

Bielski, B. H. J., Cabelli, D. E., Arudi, R. L., and Ross, A. B.: Reactivity of HO_2/O^{-2} Radicals in Aqueous Solution, J. Phys. Chem. Ref. Data, 14, 1041-1100, 1985.

Canonica, S., Hellrung, B., Wirz, J.: Oxidation of phenols by triplet aromatic ketones in aqueous solution, J. Phys. Chem. A, 104, 1226-1232, 2000.

Choi, S., Baik, S., Park, S., Park, N., and Kim, D.: Implementation of Differential Absorption LIDAR (DIAL) for Molecular Iodine Measurements Using Injection-Seeded Laser, J. Opt. Soc. Korea, 16, 325-330, 2012.

Corral-Arroyo, P., Bartels-Rausch, T., Alpert, P. A., Dumas, S., Perrier, S., George, C., and Ammann, M.: Particle phase photosensitized radical production and aerosol aging, Env. Sci. Technol., 52 (14), 7680–7688, 2018.

González Palacios, L., Corral Arroyo, P., Aregahegn, K. Z., Steimer, S. S., Bartels-Rausch, T., Nozière, B., George, C., Ammann, M., and Volkamer, R.: Heterogeneous photochemistry of imidazole-2-carboxaldehyde: HO_2 radical formation and aerosol growth, Atmos. Chem. Phys., 16, 11823-11836, 2016.

Ishigure, K., Shiraishi, H., and Okuda, H.: Radiation-chemistry of aqueous iodine systems under nuclear-reactor accident conditions, Rad. Phys. Chem., 32, 593-597, 1988.

IvkovicJensen, M. M. and Kostic, N. M.: Effects of viscosity and temperature on the kinetics of the electron-transfer reaction between the triplet state of zinc cytochrome c and cupriplastocyanin, Biochem., 36, 8135-8144, 1997.

Kunze, A., Muller, U., Tittes, K., Fouassier, J. P., and MorletSavary, F.: Triplet quenching by onium salts in polar and nonpolar solvents, J. Photochem. Photobiol. A-Chem., 110, 115-122, 1997.

Lamola, A. A. and Hammond, G. S.: Mechanisms of Photochemical Reactions in Solution. XXXIII. Intersystem Crossing Efficiencies, J. Chem. Phys, 43, 2129-2135, 1965.

Lienhard, D. M., Huisman, A. J., Bones, D. L., Te, Y. F., Luo, B. P., Krieger, U. K., and Reid, J. P.: Retrieving the translational diffusion coefficient of water from experiments on single levitated aerosol droplets, Physical chemistry chemical physics : Phys. Chem. Chem. Phys., 16, 16677-16683, 2014.

Maillard, B., Ingold, K. U., and Scaiano, J. C.: Rate constants for the reactions of free-radicals with oxygen in solution, J. Am. Chem. Soc., 105, 5095-5099, 1983.

Mitroka, S., Zimmeck, S., Troya, D., and Tanko, J. M.: How Solvent Modulates Hydroxyl Radical Reactivity in Hydrogen Atom Abstractions, J. Am. Chem. Soc., 132, 2907-2913, 2010.

Morrison, M., Bayse, G. S., and Michaels, A. W.: Determination of spectral properties of aqueous I_2 and I_3^- and equilibrium constant, Anal. Biochem., 42, 195, 1971.

Nagarajan, V. and Fessenden, R. W.: Flash-photolysis of transient radicals. 1. Cl_2^-, Br_2^-, I_2^- and SCN_2 J. Phys. Chem., 89, 2330-2335, 1985.

Schwarz, H. A. and Bielski, B. H. J.: Reactions of HO_2 and O_2^- with iodine and bromine and the I_2^- and i atom reduction potentials, J. Phys. Chem., 90, 1445-1448, 1986.

Tinel, L., Dumas, S., and George, C.: A time-resolved study of the multiphase chemistry of excited carbonyls: Imidazole-2-carboxaldehyde and halides, C. R. Chimie, 17, 801-807, 2014.

Wagner, I. and Strehlow, H.: On the flash-photolysis of bromide ions in aqueous solutions, Ber. Bunsen-Ges. Phys. Chem. Chem. Phys., 91, 1317-1321, 1987.